Archives of Biochemistry and Biophysics 688 (2020) 108370

Contents lists available at ScienceDirect

Archives of Biochemistry and Biophysics

journal homepage: www.elsevier.com/locate/yabbi

The high-resolution crystal structure of lobster hemocyanin shows its enzymatic capability as a phenoloxidase

Taro Masuda[a,*], Seiki Baba[b], Koichi Matsuo[c], Shinji Ito[d,1], Bunzo Mikami[e,f]

[a] Laboratory of Marine Biology, Division of Applied Biological Science, Faculty of Agriculture, Setsunan University, 45-1 Nagaotoge-cho, Hirakata, Osaka, 573-0101, Japan
[b] Protein Crystal Analysis Division, Japan Synchrotron Radiation Research Institute (JASRI/SPring-8), 1-1-1 Kouto, Sayo, Hyogo, 679-5198, Japan
[c] Hiroshima Synchrotron Radiation Center, Hiroshima University, 2-313 Kagamiyama, Higashi-Hiroshima, Hiroshima, 739-0046, Japan
[d] Medical Research Support Center, Graduate School of Medicine, Kyoto University Yoshida Konoe-cho, Sakyo-ku, Kyoto, 606-8501, Japan
[e] Laboratory of Applied Structural Biology, Division of Applied Life Sciences, Graduate School of Agriculture, Kyoto University, Gokasho, Uji, Kyoto, 611-0011, Japan
[f] Laboratory of Metabolic Science of Forest Plants and Microorganisms, Research Institute for Sustainable Humanosphere and Laboratory of Structural Energy Bioscience, Institue of Advance Energy, Kyoto University, Gokasho, Uji, Kyoto, 611-0011, Japan

ARTICLE INFO

Keywords:
Type 3 copper protein
Hemocyanin
Phenoloxidase
Arthropod
Crustacean

ABSTRACT

Hemocyanin (Hc) and phenoloxidase (PO) are members of the type 3 copper protein family. Although arthropod Hc and PO exhibit similar three-dimensional structures of the copper-containing active site, Hc functions as an oxygen transport protein, showing minimal or no phenoloxidase activity. Here, we present the crystal structure of the oxy form of Hc from *Panulirus japonicus* (PjHc) at 1.58 Å resolution. The structure of the di-copper active site of PjHc was found to be almost identical to that of PO. Although conserved amino acids and the water molecule crucial for the enzymatic activity were observed in PjHc at almost the same positions as those in PO, PjHc showed no enzymatic activity under our experimental conditions. One striking difference between PjHc and arthropod PO was the presence of a "blocker residue" near the binuclear copper site of PjHc. This blocker residue comprised a phenylalanine residue tightly stacked with an imidazole ring of a CuA coordinated histidine and hindered substrates from accessing the active site. Our results suggest that the blocker residue is also a determining factor of the catalytic activity of type 3 copper proteins.

1. Introduction

Hemocyanin (Hc) is a member of the family of type 3 copper proteins, which is characterized by binuclear copper atoms, each of which is coordinated by three histidine side chains [1]. In general, Hc is abundant in the hemolymph of arthropods and mollusks, and functions as a dioxygen-transporting protein. Although Hc from both arthropods and mollusks share common structural features, namely the copper center where dioxygen is reversibly bound as peroxide in side-on bridging coordination, the structural basis of the Hc molecule as a whole between arthropods and mollusks is far less conserved [2]. Molluscan Hc forms a huge cylindrical supermolecule composed of decameric or multidecameric 330 to 450-kDa subunits. Each subunit has a subset of approximately 50-kDa sequentially arranged paralogous functional units that contain a type 3 copper center [3]. In contrast, a subunit of arthropod Hc is approximately 75-kDa and is composed of three domains, among which the binuclear copper center is found in domain II. Each subunit assembles to form a hexamer, the basic unit of arthropod hemocyanin. These hexamers sometimes gather to form a larger structure, such as a dodecamer or higher aggregates [4].

The structure of the arthropod Hc subunit is rather similar to that of arthropod phenoloxidase (PO), another member of the family of type 3 copper proteins. Arthropod proPO catalyzes the key reactions of melanin formation, i.e. the hydroxylation of monophenols to *o*-diphenols (monophenolase activity; E.C. 1.14.18.1) and the subsequent oxidation to the corresponding quinone (diphenolase [catecholoxidase] activity; E.C. 1.10.3.1). Proteins with those enzymatic activities are ubiquitously distributed in bacteria, fungi, plants, and vertebrates, for example, tyrosinases and polyphenoloxidases (PPO) with both mono- and diphenolase activities, and catechol oxidases (CO) with only diphenolase

* Corresponding author. Tel.: +81 72 896 5486.
E-mail addresses: taro.masuda@setsunan.ac.jp, taro.masuda@setsunan.ac.jp (T. Masuda), baba@spring8.or.jp (S. Baba), pika@hiroshima-u.ac.jp (K. Matsuo), ito.shinji.3v@kyoto-u.ac.jp (S. Ito), mikami.bunzo.2v@kyoto-u.ac.jp (B. Mikami).
[1] Current address: Bunzo Mikami, Laboratory of Metabolic Science of Forest Plants and Microorganisms, Research Institute for Sustainable Humanosphere and Laboratory of Structural Energy Bioscience, Institue of Advance Energy, Kyoto University, Gokasho, Uji, Kyoto, 611-0011, Japan.

https://doi.org/10.1016/j.abb.2020.108370
Received 13 February 2020; Received in revised form 7 April 2020; Accepted 8 April 2020
Available online 05 May 2020
0003-9861/

List of abbreviations

Hc	hemocyanin
proPO	pro-phenoloxidase
PO	phenoloxidase
PDB	Protein data bank
CD	Circular dichroism

activity [5,6]. The overall structures of tyrosinases, PPO, and CO from bacteria, fungi, and plants are closely related to that of the functional unit of molluscan Hc, whereas these proteins are structurally distinct from Hc and PO from arthropods [6,7]. However, the structures of the copper-containing active site are comparable among these type 3 copper proteins.

The arthropod proPO system is a major component of the innate immunity of arthropods, as quinone species (the reactive intermediate of this enzymatic reaction) are harmful to pathogenic bacteria and fungi. PO also contributes to the physical encapsulation of pathogens and wound healing by producing melanin [8]. Molecular evolutionary studies and phylogenic analyses of the primary structures of arthropod Hc and PO suggest that they are derived from a common ancestral protein with enzymatic activity, and that Hc eventually lost its PO activity and became specialized as an oxygen-transporting protein [9–11]. However, significant or trace PO activity of some arthropod hemocyanins has been reported [12–16].

Due to the extreme abundance and biological significance of Hc, the structural analysis of arthropod Hc has a very long history. Crustacean Hc is one of the first multimeric proteins, the crystal structure of which was solved by X-ray crystallography [17–20]. The first determined crystal structure of Hc is from a crustacean, the California spiny lobster (*Panulirus interruptus*), at 3.2 Å resolution (PDB ID: 1HC1 and 1HCY) [19]. The crystal structure of arthropodan Hc from the horseshoe crab (*Limulus polyphemus*), an ancient arthropod that belongs to the subphylum of chelicerates, was later solved at 2.18–2.4 Å resolution (PDB ID: 1LLA, 1NOL and 1OXY) [21,22].

Although these crystal structures contributed significantly to the establishment of the mechanisms underlying the oxygen binding and transition between the oxygenated and deoxygenated states, the high-resolution crystal structure of arthropodan Hc had not been obtained to date, partially due to the complexity and heterogeneity of the Hc subunits. In contrast, the structural information of the other type 3 copper protein, POs (e.g. tyrosinases from bacteria [23–26], PPO from plants [27–31], proPO from arthropod [32–34], and catecholoxidases from plants and fungi [28,35]), was obtained in recent decades. These studies have shed light on the reaction mechanisms of mono- and di-PO reactions and provided an insight into the fundamental question concerning the functional diversity among these proteins despite the striking structural similarity of their binuclear copper centers.

The importance of the conserved asparagine and glutamate residues and water molecule around the copper site has been highlighted by several research groups, based on the structural analyses of bacterial tyrosinases [5,29,36,37]. These three elements are commonly observed in tyrosinases and POs with enzymatic activity, and are suggested to be crucial elements for the *o*-hydroxylation of mono-phenolic substrates. Although some exceptions have been reported in plant PPOs [38,39], the significance of these elements are further supported by the structural study of arthropod PO from a mosquito [34]. In the present study, we determined the high-resolution crystal structure of oxy-form Hc from the Japanese spiny lobster (*Panulirus japonicus*) (PjHc). PjHc had the conserved asparagine and glutamate residues and water molecule around the copper site at almost exactly the same positions as those in the proPO structures. However, there was a striking structural difference between PjHc and a proPO from a crustacean: the blocker residue phenylalanine (Phe371) stacked with a CuA-coordinated histidine (His198) side chain. This blocker phenylalanine seems to restrict the space of the cavity around the active site and hinder the access of substrates to the copper center. This crystal structure shows the significance of the blocker residue in the enzymatic activity of type 3 copper proteins, in addition to the elements highlighted earlier.

2. Materials and methods

2.1. cDNA cloning

Total RNA was extracted from the hepatopancreas of *P. japonicus* (Japanese spiny lobsters) using Sepasol RNA extraction reagent (Nacalai Tesque, Kyoto, Japan), followed by mRNA purification using Oligotex dT-30 (Takara, Ohtsu, Japan). A reverse transcription polymerase chain reaction (PCR) was performed using an oligo dT adaptor primer containing the M13M4 or T7 promoter sequence and a PrimeScript RT-PCR Kit (Takara) according to the manufacturer's instruction.

We designed gene-specific primer sets for the amplification of the partial sequence of PjHc (the primer sets of PjHc_first and PjHc_nested; Table S1) from the multiple alignments of cDNA sequences of hemocyanins from a crustacean, a closely related species to Japanese spiny lobsters. The PCR fragment (approximately 1700 bp) was amplified by the nested PCR, cloned into pMD vector (Takara), and sequenced. Subsequently, 5′- and 3′-RACE (rapid amplification of cDNA ends) were performed using a SMARTer RACE 5′/3′ kit (Clontech, Mountain View, CA). The primer sets shown in Table S1 were designed according to the partial DNA sequences of PjHc. The DNA sequences obtained from the first round of PCR and the 5′-/3′-RACE reactions were assembled to a full-length cDNA of PjHc (GenBank accession no. LC509010).

Finally, full-length cDNAs of PjHc were amplified by PCR using gene-specific primer sets specific to the sequences of the 5′- and 3′-untranslated regions and cloned into pMD vector to determine the full cDNA sequences of PjHc. Four additional independent cDNA sequences for PjHc with a high similarity to the determined primary structure of PjHc were obtained (GenBank accession nos. LC505512, LC505512, LC505513, LC505514, and LC509010).

2.2. Purification and crystallization of PjHc

PjHc was purified from the hemolymph of live Japanese spiny lobsters. The method for withdrawing the hemolymph, the salting out of the proteins, and purification with a first anion exchange chromatography was as described [40]. After the anion exchange chromatography, Hc-containing fractions without proPO were collected and concentrated using a VivaSpin 20 centrifugal concentrator (Sartorius, Göttingen, Germany). Finally, PjHc was purified with size exclusion chromatography using a Superdex 200 pg column (GE Healthcare, Buckinghamshire, UK) that was pre-equilibrated with a buffer (10 mM TrisHCl pH 7.5 containing 0.15 M NaCl). The N-terminal amino acid sequence was determined using a Procise HT automated N-terminal sequence analyzer (Applied Biosystems, Foster City, CA). The purified PjHc was further analyzed by liquid chromatography-tandem mass spectrometry (LC-MS/MS) to determine the primary structure.

The concentration of purified PjHc was determined with a spectrophotometer (UV 2550, Shimadzu, Kyoto, Japan) with the absorbance at 280 nm. The extinction coefficient of the protein was estimated based on the deduced amino acid sequence (GenBank acc. no. LC505511) using the ProtParam tool (http://web.expasy.org/protparam/). Purified PjHc was concentrated to 15 mg/ml using a VivaSpin centrifugation concentration tube.

The initial screening for the crystallization conditions was performed using a mosquito® crystallization robot (TTP Labtech, Hertfordshire, UK) at 20 °C. The initial crystallization conditions were further optimized by using the Additive Screen library of reagent (Hampton Research, Aliso Viejo, CA). Finally, the optimized

crystallization drops were prepared by mixing equal volumes of mother liquid (0.1 M Lithium sulfate monohydrate, 0.1 M Sodium citrate tribasic dihydrate pH 5.5, 20% w/v Polyethylene glycol 1000 (Hampton Research) and 10 mM $MgCl_2$) and protein solution containing 15 mg/ml of purified PjHc. Orthorhombic crystals belonging to the space group of $C222_1$ appeared within 10 days at 20 °C.

2.3. Liquid chromatography-tandem mass spectrometry (LC-MS/MS)

Purified PjHc (2 μg) was dissolved in aqueous solution containing ammonium bicarbonate (30 mM) and urea (6 M) and then reductively alkylated with dithiothreitol (5 mM) and iodoacetamide (10 mM). The alkylated solution was diluted with 4 vol of 30 mM ammonium bicarbonate and trypsinized overnight. The digestion products were purified using a C-18 spin column (Thermo Fisher Scientific, Waltham, MA) and resuspended in 0.1% formic acid. The tryptic digest (200 ng) was separated using a NanoLC Ultra 2D-plus HPLC plus equipped with a cHiPLC Nanoflex column (Eksigent, Dublin, CA) in trap-and-elute mode, with a trap column (200 μm × 0.5 mm ChromXP C18-CL 3 μm 120 Å; Eksigent) and an analytical column (75 μm × 15 cm ChromXP C18-CL 3 μm 120 Å; Eksigent). The analytical column temperature was set to 40 °C.

The separation was carried out with a binary gradient with solvent A (98% water, 2% acetontrile, 0.1% formic acid) and solvent B (20% water, 80% acetonitrile, 0.1% formic acid). The gradient program was 2%–40% solvent B for 50 min, 40%–90% B for 1 min, 90% solvent B for 5 min, 90%–2% solvent B for 0.1 min, and 2% solvent B for 18.9 min, at 300 nL/min. The eluates were infused on-line to a mass spectrometer (TripleTOF 5600+ System with NanoSpray III source and heated interface, SCIEX, Framingham, MA) and ionized in an electrospray ionization-positive mode.

The data acquisition was carried out by an information-dependent acquisition method. The acquired datasets were analyzed by ProteinPilot software, ver. 4.5beta (SCIEX), with the NCBInr database (June 2016) appended with known common contaminants (SCIEX) and four PjHc amino acid sequences deduced from the four independent cDNA clones we obtained (GenBank acc. nos. LC505511, LC505512, LC505513, and LC505514). The quality of the database search was confirmed by a false discovery rate analysis in which the reversed amino acid sequences were used as a decoy. The peptide identifications were evaluated by the MS/MS spectrum and confidence score (SCIEX). Peptides identified with ≥95% confidence were considered significant.

2.4. Data collection and refinement

We initially collected the X-ray diffraction data under flash cooling with liquid nitrogen using 20% (v/v) ethylene glycol (EG) as a cryoprotectant. However, the diffraction data were collected only up to 2.4 Å at the SPring-8 BL-38B1 facility, despite elaborate screening for appropriate cryoprotectants. Subsequently, we investigated whether the use of the humid air and glue-coating (HAG) method could improve the quality of the data (HAG experiments [41]). The aqueous glue solution consisted of 5% (w/v) polyvinyl alcohol (PVA4500; Japan VAM & POVAL Co., Osaka, Japan) and 10% (v/v) EG. The humidity control apparatus used was a HUM-1F model (Rigaku Co., Tokyo).

PjHc crystals were soaked in reservoir solution containing 5% (v/v) EG. A small amount of the glue solution was applied to and spread over a crystal mounting loop (LithoLoops; Protein Wave Co., Nara, Japan). Each crystal was directly fished up from the soaked solution using the glue-coated loop. The loop was set on a diffractometer blowing air at 93% relative humidity (RH). After 5 min, the humidity was changed to 90% RH and maintained at this value for 15 min. Then, the PjHc crystals were flash-cooled by switching from the humid air to cryo-gas at 100 K. As a result, the resolution was improved to 1.58 Å (Table 1).

The diffraction data were processed using orthorhombic crystal settings (space group $C222_1$, a = 119.45 Å, b = 207.60 Å, c = 187.36 Å, α = β = γ = 90°) and the XDS software package [42]. The initial phases were determined by molecular replacement in Molrep software [43] using the coordinates of the California spiny lobster (PDB ID. 1HCY) whose amino acid sequence shares 89.8% identity with PjHc (GenBank acc. No. LC505511). The data collection and refinement statistics are summarized in Table 1.

The initial model – the amino acid sequence was substituted by that from the assembled cDNA sequence of PjHc (GenBank accession no. LC505511) – was visualized and rebuilt using the graphic software program COOT 0.7 and further modified on sigma-weighted (2 $|F_o|$-$|F_c|$) and ($|F_o|$-$|F_c|$) electron density maps. The model was then refined in REFMAC5 program [44] from the CCP4i suite of programs (ver. 1.4.4). The amino acid sequence was partially modified according to the generated electron density map and amino acid sequences deduced from the cDNA sequences obtained herein.

After repeated model rebuilding and refinement, the final model was refined in PHENIX software [45] at 1.58 Å resolution, including anisotropic B-factor refinement. During the refinement process, the di-copper sites were refined using a model containing two coppers and a water molecule without any restraints. As a result, R_{work} dropped to 0.1489 for all 615,193 reflections and R_{free} dropped to 0.1862 for all 30,282 reflections (Table 1). Figs. 1–3 and 6 and 7 were created using the PyMOL molecular visualization system (DeLano Scientific, San Carlos, CA). The secondary structures were assigned by using the DSSP program [46].

2.5. Enzymatic assay conditions

We evaluated the enzymatic activity of PjHc by using tyramine (for

Table 1
Crystallographic statistics.

Data Collection	
X-ray source	SPring-8 BL38B1
Detector	MAR225HE
Wave length (Å)	1.0000
Resolution (Å)	50.00–1.58 (1.68–1.58)
Space group	$C222_1$
Unit cell parameters	
a (Å) =	119.45
b (Å) =	207.60
c (Å) =	187.36
Total reflections	2,326,453 (370,011)
Unique reflections	615,236 (99005)
Completeness (%)	99.7 (99.2)
Redundancy	3.78 (3.74)
Mean I/σ (I)	15.24 (2.08)
R_{merrge}	0.056 (0.464)
R-meas	0.054 (0.702)
$CC^{1/2}$ (highest resolution shell)	0.754
Refinement	
Resolution (Å)	50.0-1.58 (1.60- 1.58)
R_{work}/R_{free}	0.1489/0.1862 (0.2829/0.3492)
No. of atoms/Bfactors ($Å^2$)	
Protein	17,733/26.33
Ligands	
Ethylene glycol	17/32.43
magnesium	2/35.04
sulfate	3/34.27
Water	1324/30.77
RMSD from ideal geometry	
Bond lengths (Å)	0.006
Bond angles (degree)	0.795
Coordinate error (Å)	0.19
Ramachandran plot	
Favored regions (%)	97.8
Allowed regions (%)	2.10
Outliners (%)	0.10
PDB code	6L8S

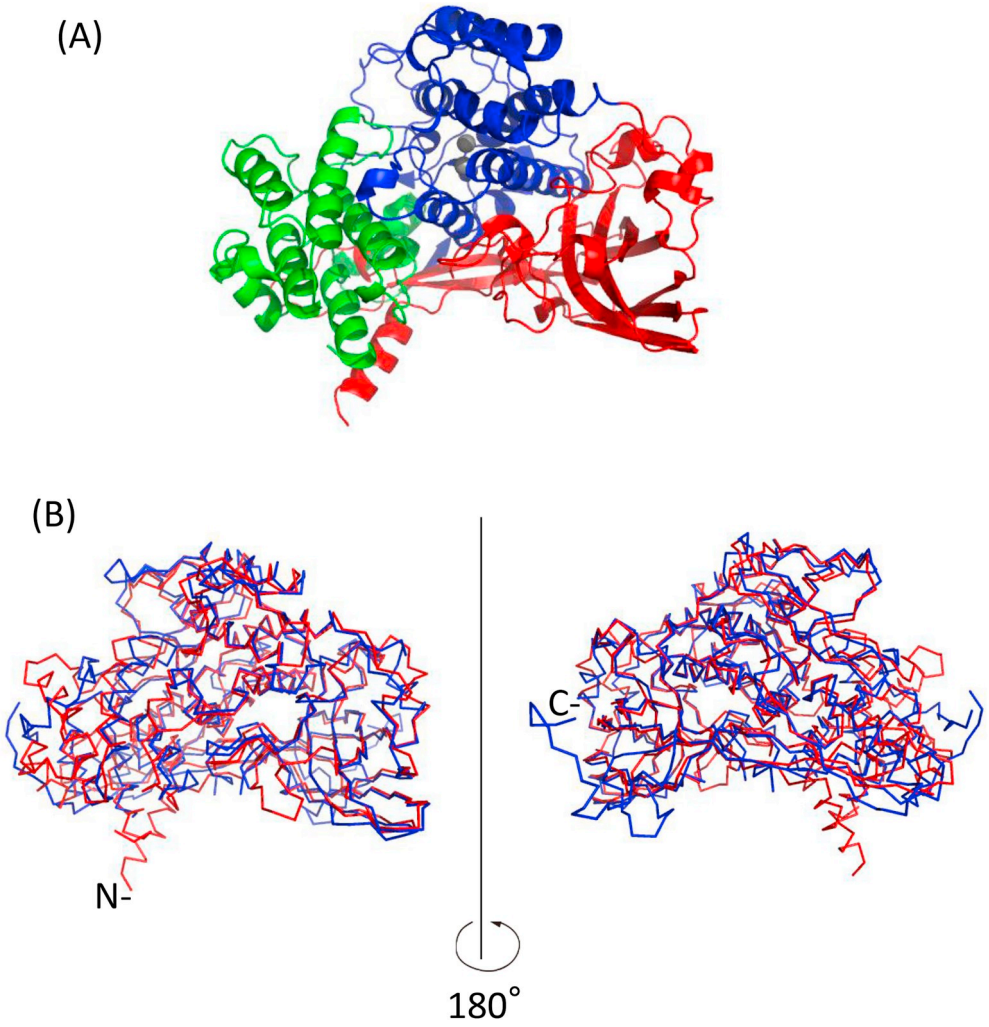

Fig. 1. The monomeric structure of PjHc. **a:** Ribbon diagram of a monomer of PjHc. Domain I, II and III are shown in *green*, *blue* and *red*, respectively. Two copper atoms in the active site (CuA, *lower* and CuB, *upper*) are shown as *gray balls*. **b:** Main chain super imposition model of PjHc (*red*) and MjproPOβ (*blue*). Viewed from two different angles (180° rotaion).

mono-PO activity) and dihydroxyphenylalanine (DOPA) (for di-PO activities) as substrates. The purified proPO (α-type) from the Japanese spiny lobster [40] and β-type from the kuruma prawn were used as a positive control. Each reaction mixture was composed of a 5.0 mM substrate, 20 mM Tris HCl (pH 7.5), 0.15 M NaCl, and 0.1% (w/v) SDS. The enzymatic reaction was initiated by the addition of purified proteins (PjHc and PjproPO) to 200 μL of the reaction mixture. The final concentration of each protein was 0.60 mg/ml (8.0 μM, PjHc) and 3.0 μg/ml (40 nM, PjproPO), respectively. The molar concentration of PjproPO was estimated using the sequence of a similar type of proPO from *M. japonicus*. The formation of dopachrome was monitored at 490-nm absorbance using a microplate reader (Sunrise; Tecan, Männedorf, Switzerland).

2.6. Circular dichroism spectroscopy using synchrotron radiation

The circular dichroism (CD) spectra of PjHc and proPOβ in 10 mM Tris HCl (pH 7.5) were measured from 260 to 175 nm in the presence or absence of 0.1% SDS at 25 °C using a vacuum-ultraviolet CD spectrophotometer in the Hiroshima Synchrotron Radiation Center. The optical devices and sample cells of the spectrophotometer are described in detail elsewhere [47,48]. The path length of the optical cell was adjusted to 50 μm using a Teflon spacer. All of the CD spectra were recorded with a 1.0-mm slit, a 4-s time constant, a 20-nm min^{-1} scan speed, and using four accumulations. All of the CD spectra were constant within an experimental error of 5% during data acquisition, which took about 20 min.

2.7. Data availability

The atomic coordinates and structure factors for PjHc have been deposited in the Protein Data Bank (https://www.rcsb.org/) under accession code (6L8S).

3. Results and discussion

3.1. Structural analysis of PjHc

PjHc crystals were successfully obtained using purified PjHc (15 mg/ml). The initial phases of the diffraction data set were determined by molecular replacement using the coordinates of Hc from a California spiny lobster (1HCY). Subsequently, the amino acid sequence was replaced with the deduced amino acid sequence from the cDNA clone isolated from the hepatopancreas total RNA of a Japanese spiny lobster (GenBank accession no. LC509010). However, the sequence was partially mismatched to the well-refined electron density map. We then determined the N-terminal amino acid sequence of a crystallization sample as DVVASST by using a protein sequencer that corresponded to

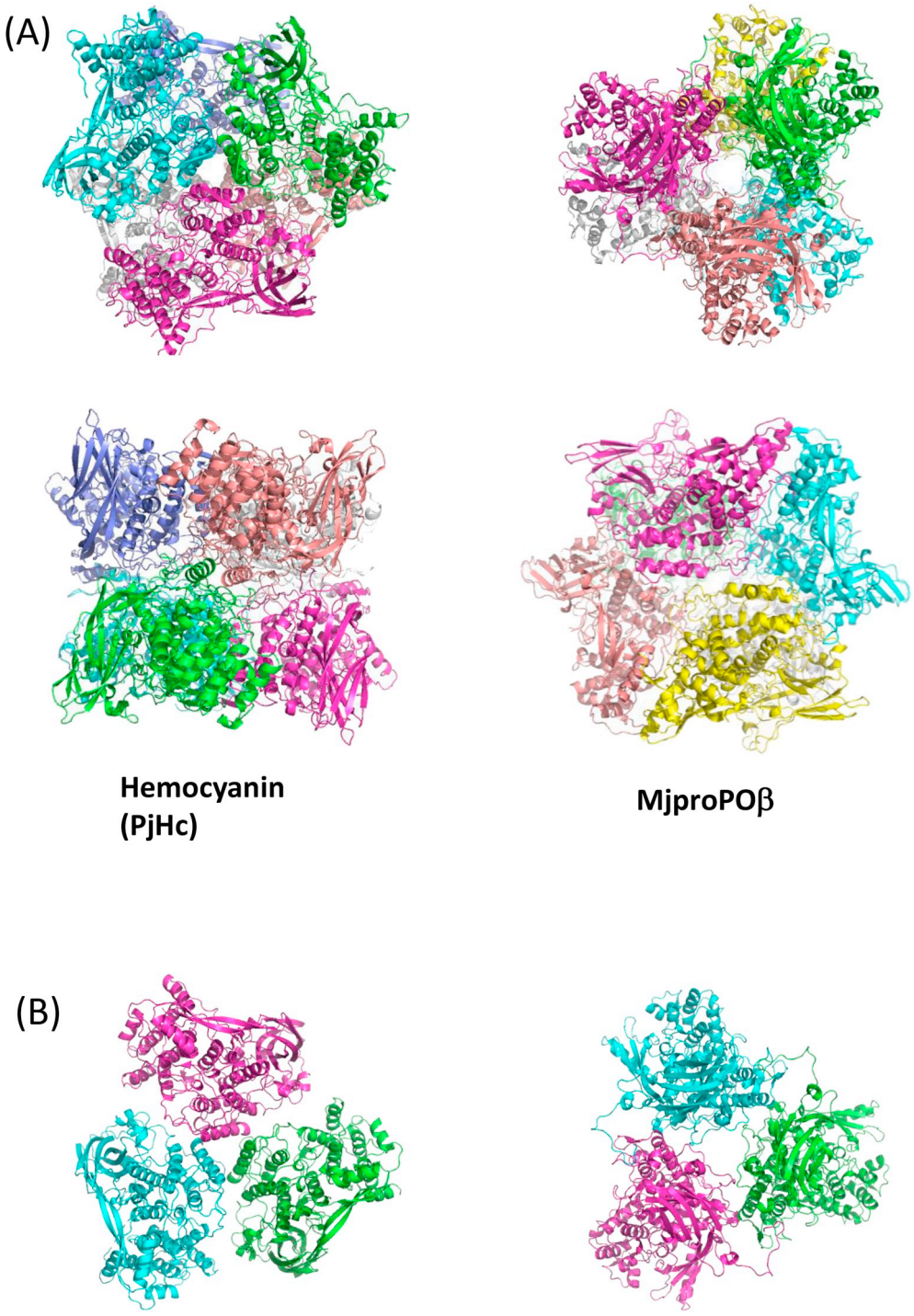

Fig. 2. Comparison of the hexameric structures of PjHc (*left*) and MjproPOβ (*right*). **a:** A hexamer of PjHc (left) and MjproPOβ (right) are viewed down a three-fold (*upper*) and two-fold (*lower*) non-crystallographic symmetry axis. Each subunit is shown in a different color. **b:** Trimeric assembly of PjHc (*left*) and MjproPOβ (*right*) viewed from a three-fold non-crystallographic symmetry axis. **c:** Schematic models (*left*) and ribbon diagram (stereo-views) (*right*) of rotation angles of two trimeric assemblies of PjHc (upper) and MjproPOβ (lower).

the sequence of a clone identified herein (GenBank accession no. LC505512), although there were still a few amino acid residues that could not be determined definitely. For examples, all the sequences determined here have leucine at 246th position, whereas the electron density map shows the shape of valine.

Similarly, peptides identified by LC-MS/MS could be assigned to one or several of the four cDNA clones (LC505511, LC505512, LC505513, and LC505514) obtained (Fig. S1); however, none of these four cDNA clones could account for all of the identified peptides. This may be due to genomic variations in the wild Japanese spiny lobsters used and/or the multiplicity of hemocyanin genes in the lobster genome. Based on these results, we attempted to align and combine the identified peptides and the amino acid sequence deduced from the four cDNA clones to estimate the full-length amino acid sequence of PjHc. This approach worked well; the estimated full-length sequence matched almost completely to the electron density map of the crystallized PjHc (PDB ID: 6L8S).

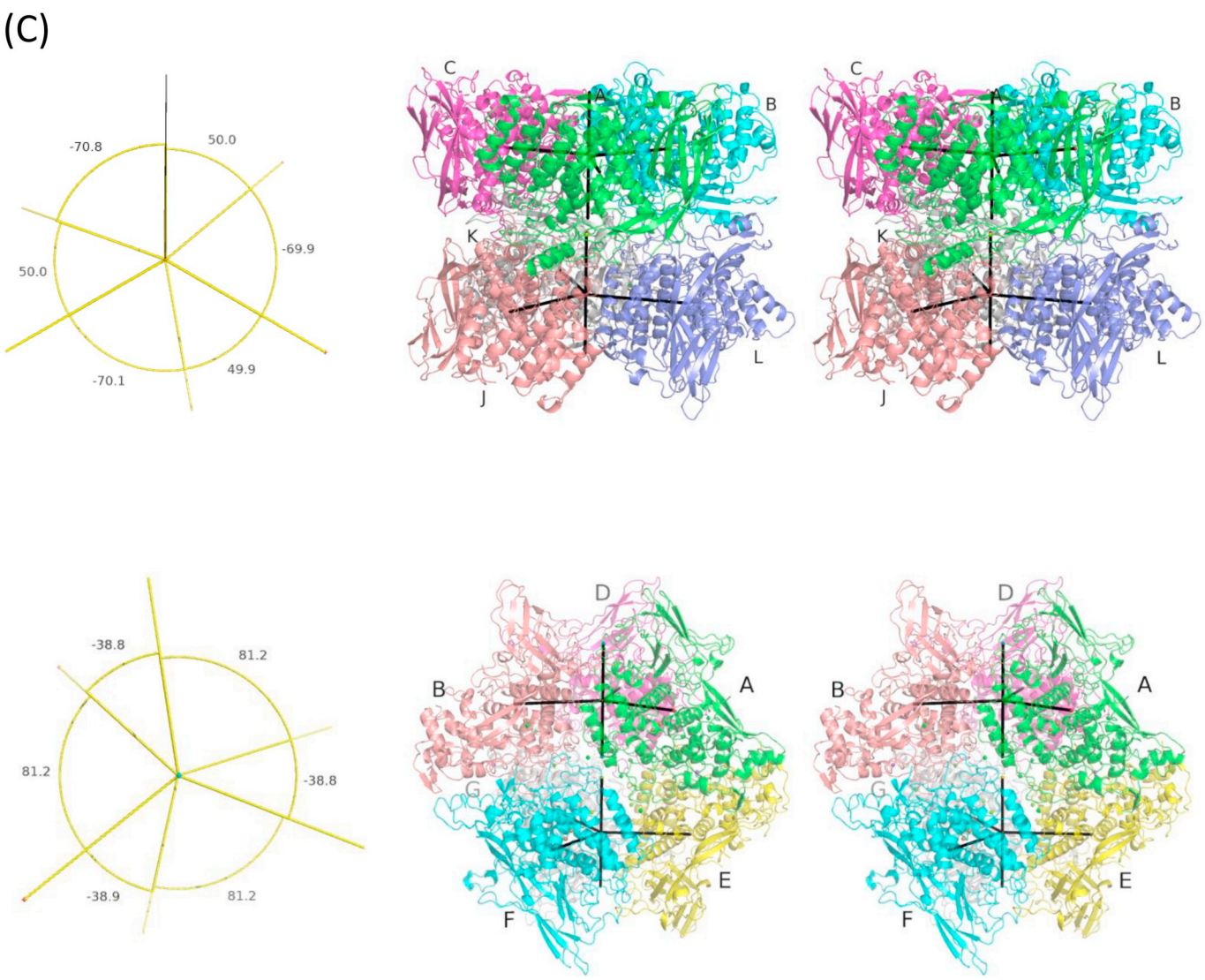

Fig. 2. (*continued*)

3.2. Hexameric structure of PjHc

Fig. 1A illustrates the monomeric structure of PjHc with domains I (shown in green), II (blue), and III (red). As shown in Fig. 1B, the structure of PjHc (shown in red) – a typical crustacean Hc – has a structure that is closely related to that of crustacean proPO (shown in blue), although the amino acid sequence identity is 30.5%. The root mean square deviation of the main chains of PjHc and MjproPOβ was calculated as 1.57 Å with 548 alignable amino acid residues out of 657 residues of which the mature region of PjHc is composed.

Fig. 2A provides the hexameric structure of PjHc (Fig. 2A, left). The crystal contained a trimer of PjHc in its asymmetric unit (Fig. 2B, left), from which the hexamer, known as a typical structure of crustacean Hc, can be generated via a crystallographic operation (Fig. 2A, left). In the hexameric structure of PjHc, two of the trimers interact to each other via face-to-face fashion with a 50° rotation around the three-fold symmetry axis (Fig. 2C, upper). As we have previously reported [33], crustacean proPO from kuruma prawn (i.e. MjproPOβ) also forms a hexamer (Fig. 2A, right). However, the quaternary assembly is remarkably different from that of PjHc; i.e. the trimeric units are assembled in a different manner (Fig. 2B), with a rotation angle of the inter-trimeric interaction in MjproPOβ that is approximately 40° (Fig. 2C, lower).

In the hexameric structure of PjHc, two trimers interact mainly in domain II of each subunit (Asn489, Lys177-Asp241, Trp239-Trp239, Asp273-Lys360, and Glu254-Lys360), whereas domains I and III contribute to the inter-trimeric interactions to form a hexamer of proPOβ. These differences in inter-subunit interactions resulted in the formation of hexameric structures of PjHc and MjproPOβ with remarkably different conformations (Fig. 2A). There is a pore along with the three-fold symmetry axis of the hexamer of PjHc and MjproPOβ (Fig. 2A, upper). The pore of PjHc has a cylindrical inner surface lined with His276, Asn294, Ile291, Arg295, Glu298, and Tyr339 side chains of approximately 7 Å dia., whereas the pore of the proPOβ hexamer is relatively large with an approximately 20 Å dia [33]. Although the large pore along the three-fold symmetry axis of proPOβ has enough size for substrates to pass through, substrates would not reach the active site from this channel. The active site seems to be more accessible from outer surface of proPOβ hexamer [33]. The buried surface areas of the dimer and trimer interfaces are 1119.8 $Å^2$ and 520.4 $Å^2$ in PjHc and 889.7 $Å^2$ and 694.5 $Å^2$ in MjproPOβ, respectively.

3.3. Structure of the copper center

The structures of the copper centers of characterized type 3 copper proteins are illustrated in Fig. 3. The structure of the copper center of PjHc is essentially identical to the structures of the reported proPOs and is similar to tyrosinases that have both mono- and di-PO activity. In

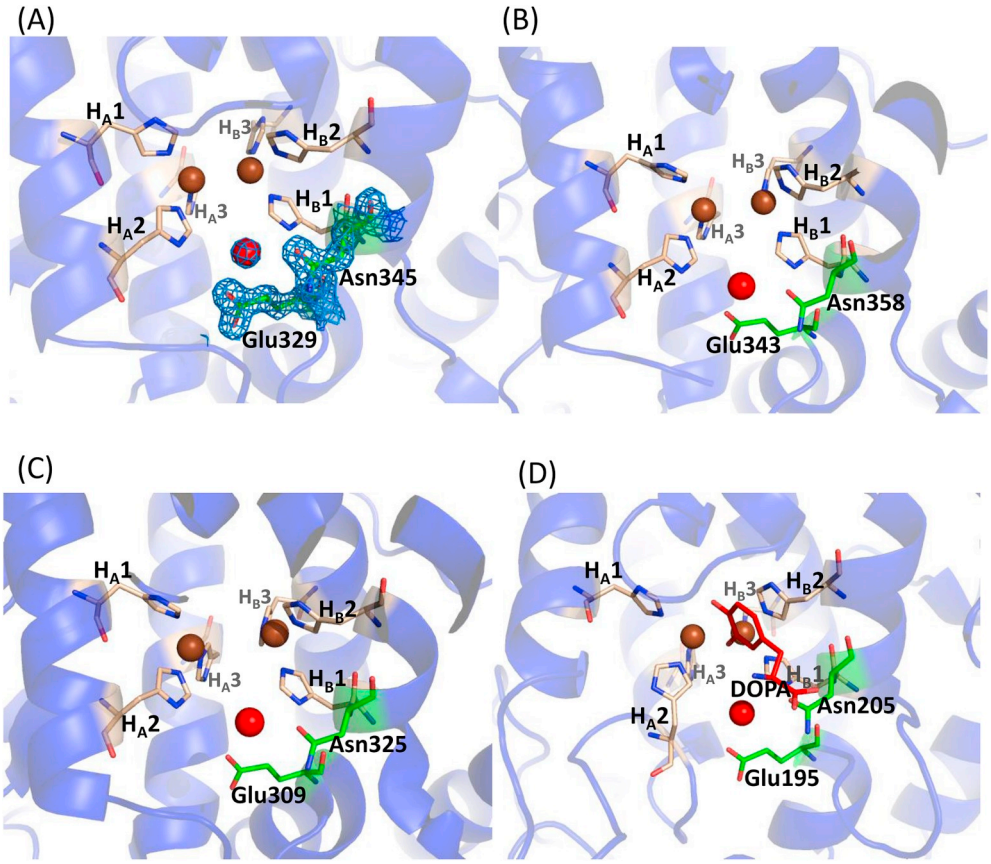

Fig. 3. The structures of the di-copper center of PjHc and other type 3 copper proteins. Type 3 copper centers of PjHc (PDB ID: 6L8S) **(a)**, proPOβ from *M. japonicus* (MjproPO) (3wky) **(b)**, proPO from *Manduca sexta* (MsproPO) (3hhs) **(c)**, and TyBM with DOPA (4p6s) **(d)**. The electron density of the 2 $|F_o|$-$|F_c|$ map for the conserved Asn, Glu, and water is contoured at 1.5σ and shown in *gray mesh* (a). Two copper atoms are shown as a *brown ball* (CuA: *left* and CuB: *right*), while the conserved water molecule is shown as a *red ball*. Six coordinated histidine residues are shown as *beige sticks*. The conserved glutamate and asparagine residues are shown as *green sticks*. DOPA is shown as a *red stick* in (d). (For interpretation of the references to color in this figure legend, the reader is referred to the Web version of this article.)

particular, the proPO from arthropods (MjproPOβ from the kuruma prawn and MsproPO from *Manduca sexta*) share a striking similarity to the structure of the copper center of PjHc (Fig. 3a–c). A brief description of the structure of the copper centers is as follows: the copper A (CuA)-coordinating histidine residues (His194, -198, and −224 in PjHc) and the copper B (CuB)-coordinating histidine residues (His344, -348, and −384 in PjHc) are called H_A1, H_A2, H_A3, H_B1, H_B2, and H_B3, respectively (Table 2). Several factors that are required for mono- and di-PO activity were reported by Goldfeder et al. [36], who determined the structures of enzyme-substrate complexes by using a tyrosinase from *Bacillus megaterium* (Tyr-Bm) and various substrates, including L-tyrosine, L-DOPA, and *p*-tyrosol. Goldfeder et al. suggested that a *p*-hydroxyl group in the substrates is directed to CuA, with the phenyl ring of the substrate stacked with the side chain imidazole ring of His208, which corresponds to H_B2 (Fig. 3d). They also suggested that the base needed for the electrophilic substitution of the *o*-hydrogen atom is a conserved water molecule that is activated by conserved glutamate (Glu195) and asparagine (Asn205) residues (Fig. 3d). These three factors (i.e. conserved water molecule, glutamate residue, and asparagine residue) are observed not only in proPOs and tyrosinases but also in enzymatically inactive PjHc. This indicates that PjHc intrinsically has the catalytic machinery needed for the enzymatic oxidation of phenolic substrates, and that there is another factor that determines whether a type 3 copper protein has apparent PO activity.

3.4. Mono- and di-PO activity of PjHc compared with proPO

To measure the mono- and di-PO activity, Hc and proPO purified from the hemolymph of the Japanese spiny lobster and the kuruma prawn were reacted with substrates for mono- and di-PO reactions. Generally, Hc is so abundant in the hemolymph of crustaceans that it is very difficult to separate Hc and proPO, which have a similar oligomeric state as hexamers, from each other [40,49]. However, our PjHc and proPOα preparations were almost pure, judging from the results of Coomassie Brilliant Blue (CBB) staining (Fig. 4a) and western blotting, using specific antibodies for crustacean proPOs.

In our experimental conditions, PjHc showed almost no detectable enzymatic activity for a mono-phenol substrate (tyramine) (Fig. 4c) and a di-phenol substrate, (DOPA; Fig. 4d), although 200-times more PjHc was used in the reactions. For further characterization of the enzymatic properties, PjHc and proPOs were separated by sodium dodecyl sulfate-polyacrylamide gel electrophoresis (SDS-PAGE) in non-reducing conditions without heat treatment and then stained using a di-phenolic substrate, DOPA (Fig. 4b). The polyacrylamide gel and the sample

Table 2
The amino acid residues corresponding to copper-coordinating histidines, “Place-holder” and “Blocker”.

	H_A1	H_A2	H_A3	H_B1	H_B2	H_B3	Place holder	Blocker
Hc (*P. japonicus*)	His194	His198	His224	His344	His348	His384	Phe75	Phe371
POβ (*M. japonicus*)	His199	His203	His226	His357	His361	His397	Phe72	Val384
PO (*M. sexta*)	His215	His219	His245	His368	His372	His408	Phe88	Glu395
Hc (*L. polyphemus*)	His173	His177	His204	His324	His328	His364	Phe49	Thr351
TyrBM (*B. megaterium*)	His42	His60	His69	His204	His208	His231	–	–
MdPPO (*M. domestic)*	His86	His107	His116	His238	His242	His272	–	Phe259

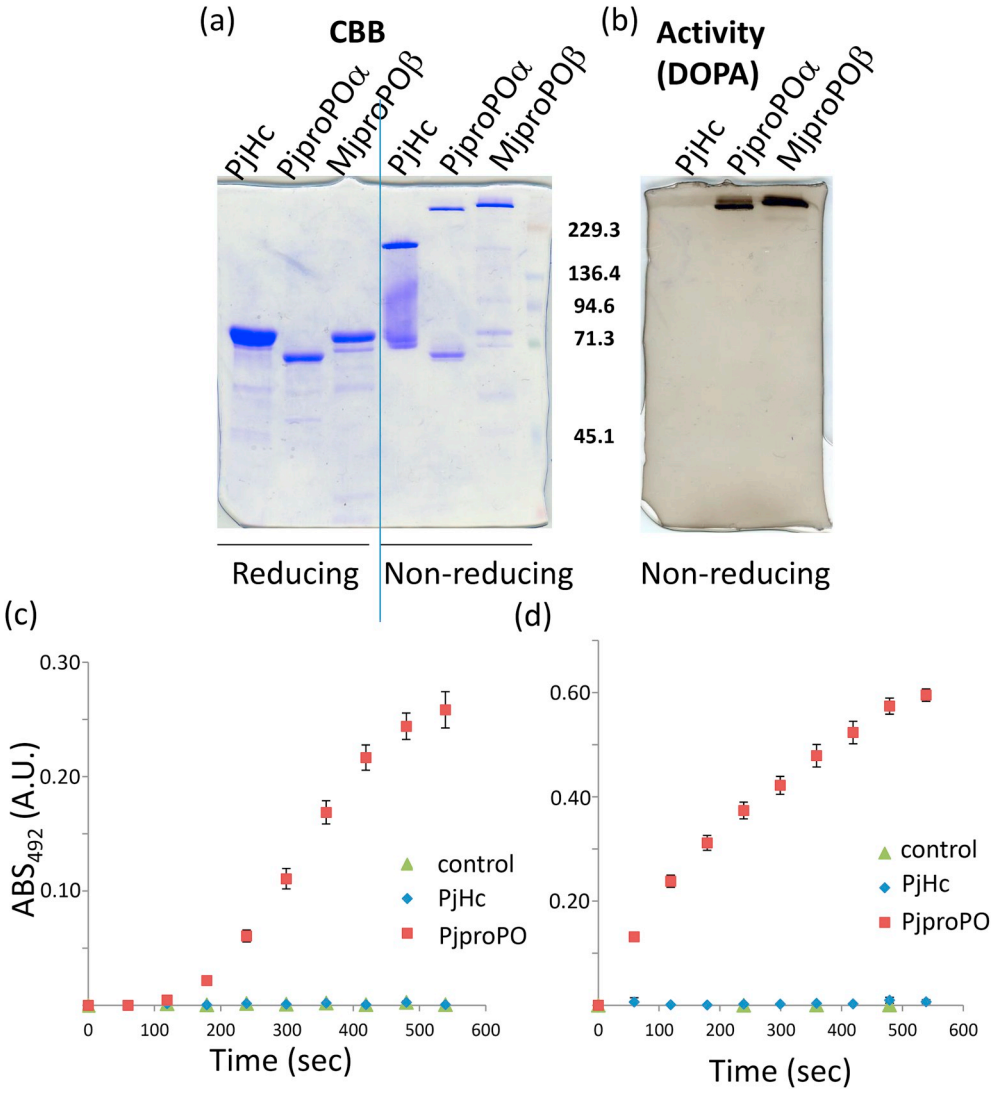

Fig. 4. The mono- and di-PO activity of PjHc and prophenoloxidases from crustacean (*P. japonicus and M. japonicus*). **a:** Reducing (left) and non-reducing without heat treatment (*right*) SDS-PAGE, followed by Coomassie Brilliant Blue staining of each preparation. The oligomeric state is maintained in the latter condition. **b:** After the separation by non-reducing SDS-PAGE (a, *right*), the gel was stained by a di-PO substrate, DOPA, by dipping the gel in the solution containing 5 mM substrate. **c:** The mono-PO (substrate: 5 mM tyramine) and (d) di-PO (substrate: 5 mM DOPA) activity of PjHc, and PjproPOα. The formation of dopachrome was monitored at 490-nm absorbance. Error bars: SE of three independent analyses. (For interpretation of the references to color in this figure legend, the reader is referred to the Web version of this article.)

buffer for SDS-PAGE contained 0.2% and 2% SDS, respectively, in addition to 0.1% SDS in the substrate mixture. However, this activity staining did not reveal a clear PjHc signal with di-PO activity. In contrast, hemolymph proPO from Japanese spiny lobster and kuruma prawn (*Marsupenaeus japonicus*; MjproPOβ) produced a prominent black band that corresponded to the proPO band of the CBB stain (Fig. 4b). These results indicated that mono- and di-PO activities of PjHc were undetectable or very low compared to those of proPOs.

3.5. Circular dichroism (CD) spectra of PjHc and proPOβ with or without SDS

To clarify whether the activity inducer (0.1% SDS) influenced the structure of PjHc and proPOβ, we analyzed the CD spectra of these proteins by using a synchrotron radiation facility. The CD spectra of each protein are shown in Fig. 5. The spectrum of PjHc in the absence of SDS exhibited two negative peaks, around 222 and 208 nm, and one positive peak, around 190 nm (Fig. 5a), which are the characteristics observed in the α-helical structures [50,51]. This was essentially identical in the presence of 0.1% SDS (Fig. 5a). The proPOβ had similar characteristic peaks with those of PjHc, although the intensity around 208 nm largely increased. The proPOβ in the presence or absence of 0.1% SDS showed similar spectra, as well as the case of PjHc (Fig. 5b). These data indicate that the overall structures of both proteins were slightly different but not affected by the addition of activity inducer SDS at this concentration (0.1%). On the other hand, Fujieda et al. showed that some structural changes were observed on CD spectra between activated and un-activated hemocyanin from swimming crab when activated using 3 M urea [15,52]. Thus, our CD data indicate that the activation conditions used here (0.1% SDS) were too mild to induce any significant changes in the structures of PjHc and MjproPOβ, despite the fact that a small structural change induced by low concentration of SDS was enough to activate MjproPOβ. These results suggest that proPOs do not require systemic structural changes for enzymatic activation, while crustacean Hc requires relatively large structural changes, which can be detected by CD measurements.

3.6. The surrounding environment of the copper center

Although various factors are required for PO activity, crustacean Hc shows only traces or no enzymatic activity. Fig. 6a describes the surrounding environments of the type 3 copper centers of PjHc (*red*) and proPO from a prawn (*yellow*) (proPOβ: PDB ID 3WKY). In the structures of arthropod Hc and proPO, histidine residues corresponding to H_B2, which has been suggested to bind to a substrate in the structure of tyrosinase from *Bacillus* [36], are shielded by the side chain of place-holder phenylalanine (Fig. 6a). However, PjHc and even MjproPOβ and MsproPO, with high PO activities, have this place-holder phenylalanine, which is tightly packed with the H_B2 histidine side chain, indicating that the place-holder phenylalanine itself does not abolish the

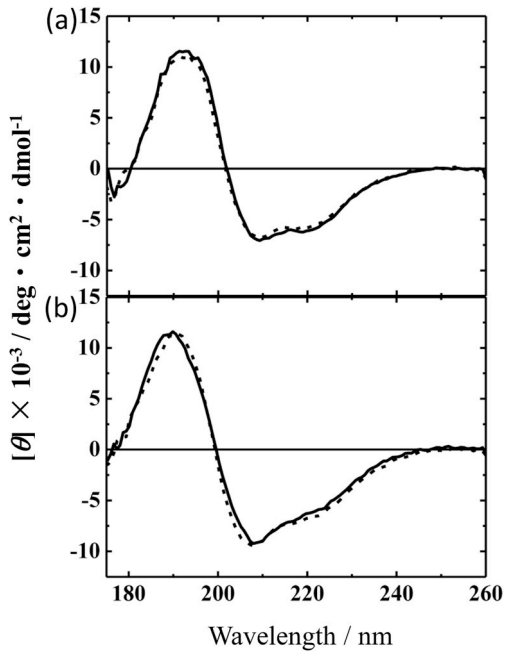

Fig. 5. CD spectra of PjHc (a) and proPOβ (b) in 10 mM Tris HCl (pH 7.5) in the absence (*solid line*) or presence of 0.1% SDS (*broken line*) at 25 °C. A cell with a path length of 50 μm was used for the measurements from 260 to 175 nm. All spectra were recorded with a 1.0-mm slit, a 4-s time constant, a 20-nm min^{-1} scan speed, and using four accumulations.

PO activity. In fact, this place-holder phenylalanine is suggested to be removed in the process of enzymatic activation [53–56].

There is another shielding residue denoted as "blocker residue" [5] (Table 2). In the structure of PjHc, the side chain of the blocker residue, Phe371, is stably stacked with the side chain of His198 (H_A2) (Fig. 6a and c). In contrast, this blocker residue is substituted by valine (Val384), threonine (Thr351), and glutamate (Glu395) in MjproPOβ, MsproPO, and LpHc (hemocyanin from *Limulus polyphemus*), respectively (Figs. 6a and 8, Table 2). As shown in Fig. 6a, this difference is most striking concerning the type 3 copper centers of arthropod Hc and PO. In terms of the function of the blocker phenylalanine, Phe371 in PjHc can be well superimposed with those of PPOs from plants (Fig. 6b) [39,57]. These authors suggested that the blocker residue does not abolish PO activity because the PPOs (MdPPO and SlPPO) have both mono- and di-PO activity. However, there are many differences between arthropod proteins (PjHc and proPOs) and plant PPOs; PPOs do not contain a place-holder residue, and the blocker phenylalanine of plant PPO is highly flexible and disordered [39], in contrast to the blocker phenylalanine in PjHc, which interacts stably with the imidazole ring of H_A2 (Fig. 6c). Therefore, we compared the structures of Hc and PO from arthropods.

Next, we investigated the effect of this difference in blocker residues between arthropod Hc and PO. The structure of MjproPOβ (PDB accession no. 3wky) has a large cavity in front of its copper center (PDB accession no. 3wky) (Fig. 7b), whereas this cavity is withdrawn by the side chain of Phe371 (the blocker residue) in the structure of PjHc (Fig. 7a). These results indicate that the accessibility of a substrate would be restricted in PjHc due to the bulky side chain of the place-holder Phe371. Indeed, this blocker phenylalanine is strictly conserved among crustacean Hcs, whereas it is substituted by less bulky amino acids in proPO and chelicerate Hcs (Fig. 8). The importance of the cavity around the active site was previously indicated in the structure of mosquito PO by Hu et al. [34].

The phenoloxidase activity of Hc is one of the most intriguing questions regarding type 3 copper proteins. Due to the extremely high similarities between the three-dimensional structures of Hc and PO

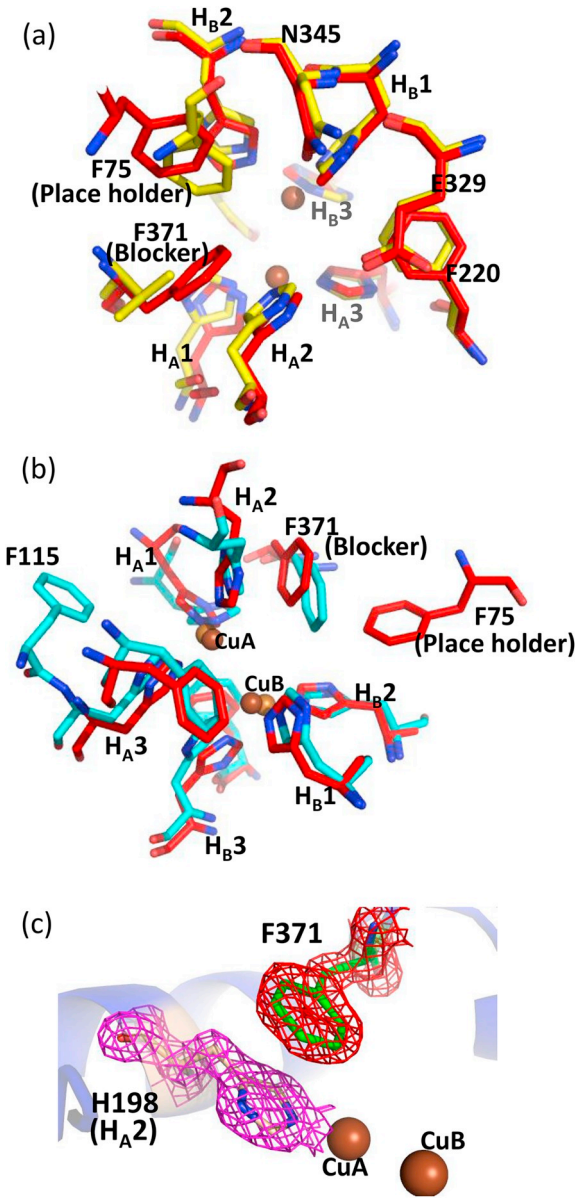

Fig. 6. Comparison of the active site structures of PjHc and MjproPOβ. **a:** Super-imposed structures of PjHc (*red*) and MjproPOβ (*yellow*). Two copper atoms are shown as *brown balls* (CuA: *lower* and CuB: *upper*). **b:** Super-imposed structures of PjHc (*red*) and MdPPO (*cyan*). (c) The interaction between the Place-holder and H_A2 (His198) in PjHc. The electron density of the 2 $|F_o|$-$|F_c|$ maps for the conserved these residues are contoured at 2.0σ and shown in *red* and *magenta mesh*.

from arthropods at the active site, it can be reasonably deduced that Hc may exert PO activity. Our structural investigation of PjHc revealed that crustacean Hc is equipped with all of the known components for gaining PO activity, although this activity was not activated under the experimental conditions used herein. One possible reason for the inactivity of crustacean Hc is the presence of a bulky blocker residue at the active site. This hypothesis would be verified by the mutational studies of PjHc and/or crustacean PO at the site of blocker residue. However, the recombinant proteins did not form correct copper site when expressed in E. coli expression system.

In recent decades, many influential studies have investigated the role of hemocyanin activation. In 1996, Nellaiappan and Sugumaran detected di-PO activity in horseshoe crab hemolymph, a finding that prompted research into the source of the PO activity in chelicerate

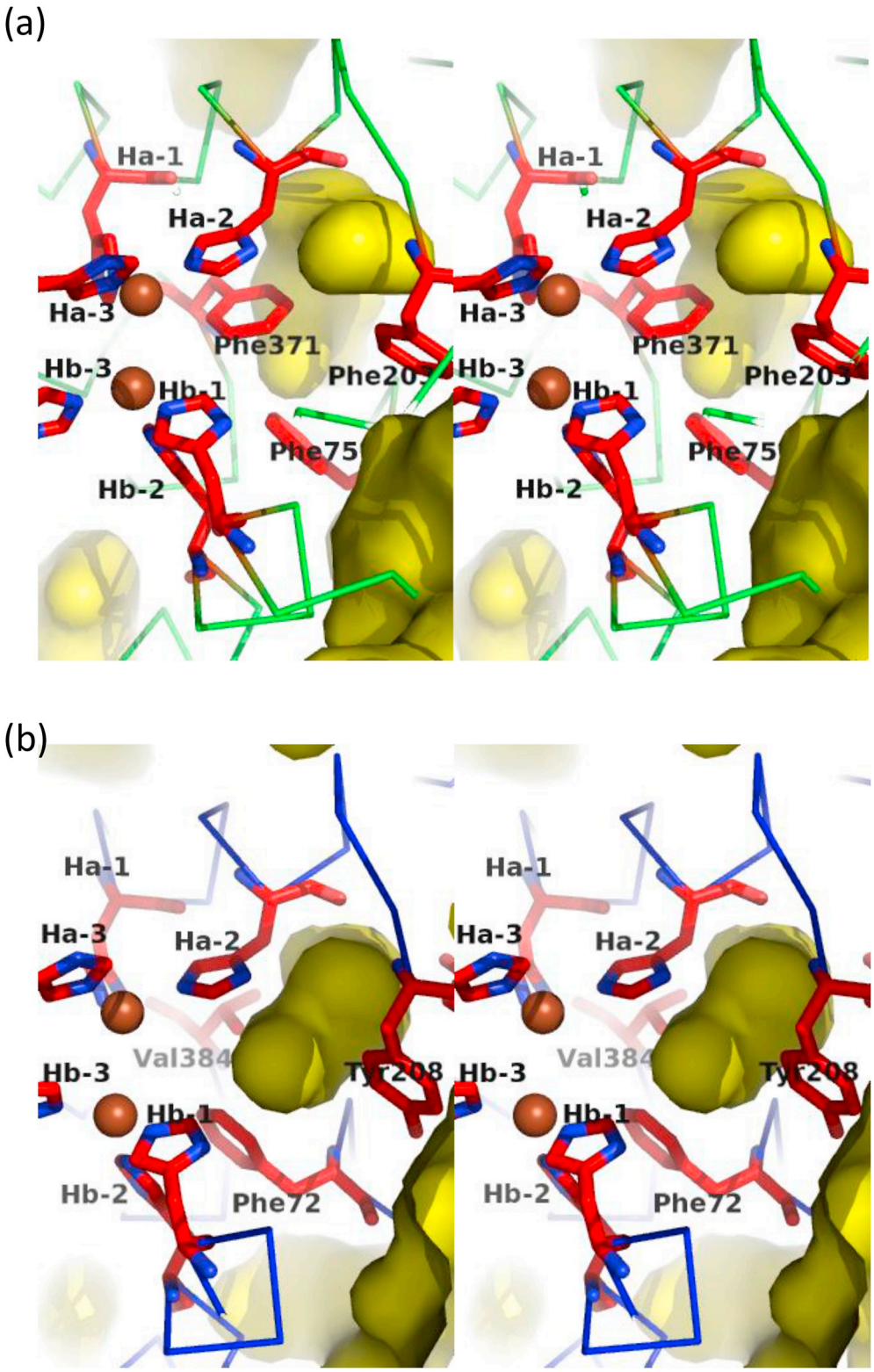

Fig. 7. Cavities are present at the active sites of PjHc **(a)** and MjproPOβ **(b)** (stereo-views). Cavities and clefts around the active sites are shown as *yellow blobs*. Coordinated histidine residues are shown as *red sticks*. Two copper atoms are shown as *brown balls* (CuA: *upper* and CuB: *lower*). (For interpretation of the references to color in this figure legend, the reader is referred to the Web version of this article.)

hemolymph [58]. In 1998, Decker and Rimke demonstrated the activation of Hc from tarantula (a chelicerate) and the subsequent ability to gain PO activity [12]. Thereafter, more sophisticated studies showed that chelicerate Hc could be converted into an active PO with di-PO activity [13,14,59]. This bi-functionality of chelicerate Hc would compensate for the hemolymph PO activity, which is one of the most important innate immunities in arthropods, since chelicerates lack the genes encoding PO [59,60].

Crustaceans have both Hc and PO in their genome, which indicates that crustacean Hc no longer needs to gain PO activity. Although di-PO

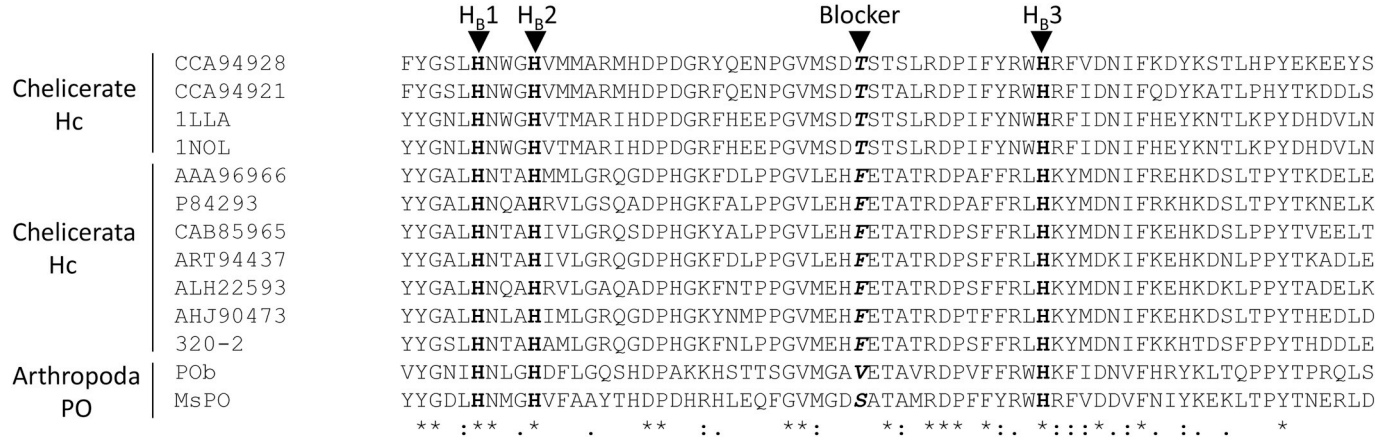

Fig. 8. Alignment of amino acid sequences around the blocker residue. Blocker residues of type 3 copper proteins from various arthropods are shown as ***bold italic***. The CuB-coordinated histidine residues are also shown in *bold*. Amino acid residues conserved among all members shown here are indicated by an *asterisk* * below the sequences.

activity has been reported in crustacean Hc, this activity is far less than that of chelicerate Hc and the true PO of crustaceans [16,60]. Regarding the mono-oxygenase activity of crustacean Hc, Fujieda et al. showed that Hc from swimming crab can gain mono-oxygenase activity under certain conditions, such as with 3 M urea (pH 9.0) borate buffer [15,52]. The research group had used urea to activate molluscan Hc [61,62].

Crustacean Hc is capable of showing clear mono- or di-PO activity under certain conditions, especially harsh conditions, such as those in which a chaotrope or a type of denaturing agent are present. We are currently investigating the conditions in which the as-of-yet undetected activity of Hc would become apparent. The possibility of the activation of crustacean Hc should be carefully considered, since Hc and PO share similar primary, three-dimensional, and tertiary structures. In addition, Hc is extremely abundant in the hemolymph of crustaceans, whereas proPO is generally less abundant. Hc and PO may contaminate and interfere with each other easily during their preparation. Taken together, our results indicate that, in the crustacean order Decapoda, the ancient hemocyanin with bifunctionality would have been specialized as an oxygen carrier by the substitution of the blocker residue during evolution.

Acknowledgements

We are grateful to Dr. Takehiko Tosha at RIKEN SPring-8 for his helpful input and support with the crystallization. The synchrotron radiation experiments were performed at beamlines BL38B1 and BL26B1 of SPring-8, with the approval of the Japan Synchrotron Radiation Research Institute (JASRI) (proposal numbers: 2017B6750, 2017A2533, 2017A2546, 2017B2547 and 2017B2546). The measurements of vacuum-ultraviolet circular-dichroism spectra were carried out with the approval of the Hiroshima Synchrotron Radiation Center of Hiroshima University (proposal number: 17AU020). This research was partially supported by Platform Project for Supporting Drug Discovery and Life Science Research (Basis for Supporting Innovative Drug Discovery and Life Science Research (BINDS)) from Japan Agency for Medical Research and Development (AMED) under Grant Number -JP18am0101070 (support number 0405). This work was financially supported by a Grant-in-Aid for Research (Grant no. 19K06221 and 17KK0154) from JSPS and by the Towa foundation for food research.

Appendix A. Supplementary data

Supplementary data to this article can be found online at https://doi.org/10.1016/j.abb.2020.108370.

References

[1] A.C. Rosenzweig, M.H. Sazinsky, Structural insights into dioxygen-activating copper enzymes, Curr. Opin. Struct. Biol. 16 (2006) 729–735.
[2] K.E. van Holde, K.I. Miller, H. Decker, Hemocyanins and invertebrate evolution, J. Biol. Chem. 276 (2001) 15563–15566.
[3] J. Markl, Evolution of molluscan hemocyanin structures, Biochim. Biophys. Acta 1834 (2013) 1840–1852.
[4] M. Beltramini, N. Colangelo, F. Giomi, L. Bubacco, P. Di Muro, N. Hellmann, E. Jaenicke, H. Decker, Quaternary structure and functional properties of Penaeus monodon hemocyanin, FEBS J. 272 (2005) 2060–2075.
[5] M. Kanteev, M. Goldfeder, A. Fishman, Structure-function correlations in tyrosinases, Protein Sci. 24 (2015) 1360–1369.
[6] E. Jaenicke, H. Decker, Functional changes in the family of type 3 copper proteins during evolution, Chembiochem 5 (2004) 163–169.
[7] E. Selinheimo, D. NiEidhin, C. Steffensen, J. Nielsen, A. Lomascolo, S. Halaouli, E. Record, D. O'Beirne, J. Buchert, K. Kruus, Comparison of the characteristics of fungal and plant tyrosinases, J. Biotechnol. 130 (2007) 471–480.
[8] L. Cerenius, B.L. Lee, K. Soderhall, The proPO-system: pros and cons for its role in invertebrate immunity, Trends Immunol. 29 (2008) 263–271.
[9] T. Burmester, K. Scheller, Common origin of arthropod tyrosinase, arthropod hemocyanin, insect hexamerin, and dipteran arylphorin receptor, J. Mol. Evol. 42 (1996) 713–728.
[10] A. Immesberger, T. Burmester, Putative phenoloxidases in the tunicate Ciona intestinalis and the origin of the arthropod hemocyanin superfamily, J. Comp. Physiol. B 174 (2004) 169–180.
[11] T. Burmester, Origin and evolution of arthropod hemocyanins and related proteins, J. Comp. Physiol. B 172 (2002) 95–107.
[12] H. Decker, T. Rimke, Tarantula hemocyanin shows phenoloxidase activity, J. Biol. Chem. 273 (1998) 25889–25892.
[13] H. Decker, M. Ryan, E. Jaenicke, N. Terwilliger, SDS-induced phenoloxidase activity of hemocyanins from *Limulus polyphemus, Eurypelma californicum*, and *Cancer magister*, J. Biol. Chem. 276 (2001) 17796–17799.
[14] T. Nagai, T. Osaki, S. Kawabata, Functional conversion of hemocyanin to phenoloxidase by horseshoe crab antimicrobial peptides, J. Biol. Chem. 276 (2001) 27166–27170.
[15] N. Fujieda, A. Yakiyama, S. Itoh, Catalytic oxygenation of phenols by arthropod hemocyanin, an oxygen carrier protein, from Portunus trituberculatus, Dalton Trans. 39 (2010) 3083–3092.
[16] T. Zlateva, P. Di Muro, B. Salvato, M. Beltramini, The o-diphenol oxidase activity of arthropod hemocyanin, FEBS Lett. 384 (1996) 251–254.
[17] B. Linzen, N.M. Soeter, A.F. Riggs, H.J. Schneider, W. Schartau, M.D. Moore, E. Yokota, P.Q. Behrens, H. Nakashima, T. Takagi, et al., The structure of arthropod hemocyanins, Science 229 (1985) 519–524.
[18] H.J. Bak, B. Neuteboom, P.A. Jekel, N.M. Soeter, J.M. Vereijken, J.J. Beintema, Structure OF arthropod hemocyanin, FEBS Lett. 204 (1986) 141–144.
[19] A. Volbeda, W.G. Hol, Crystal structure of hexameric haemocyanin from Panulirus interruptus refined at 3.2 A resolution, J. Mol. Biol. 209 (1989) 249–279.
[20] A. Volbeda, W.G. Hol, Pseudo 2-fold symmetry in the copper-binding domain of arthropodan haemocyanins. Possible implications for the evolution of oxygen transport proteins, J. Mol. Biol. 206 (1989) 531–546.
[21] K.A. Magnus, B. Hazes, H. Ton-That, C. Bonaventura, J. Bonaventura, W.G. Hol, Crystallographic analysis of oxygenated and deoxygenated states of arthropod hemocyanin shows unusual differences, Proteins 19 (1994) 302–309.
[22] B. Hazes, K.A. Magnus, C. Bonaventura, J. Bonaventura, Z. Dauter, K.H. Kalk, W.G. Hol, Crystal structure of deoxygenated Limulus polyphemus subunit II hemocyanin at 2.18 A resolution: clues for a mechanism for allosteric regulation, Protein Sci. 2 (1993) 597–619.
[23] Y. Matoba, T. Kumagai, A. Yamamoto, H. Yoshitsu, M. Sugiyama, Crystallographic

evidence that the dinuclear copper center of tyrosinase is flexible during catalysis, J. Biol. Chem. 281 (2006) 8981–8990.
[24] M. Sendovski, M. Kanteev, V.S. Ben-Yosef, N. Adir, A. Fishman, First structures of an active bacterial tyrosinase reveal copper plasticity, J. Mol. Biol. 405 (2011) 227–237.
[25] N. Fujieda, M. Murata, S. Yabuta, T. Ikeda, C. Shimokawa, Y. Nakamura, Y. Hata, S. Itoh, Activation mechanism of melB tyrosinase from Aspergillus oryzae by acidic treatment, J. Biol. Inorg. Chem. 18 (2013) 19–26.
[26] W.T. Ismaya, H.J. Rozeboom, A. Weijn, J.J. Mes, F. Fusetti, H.J. Wichers, B.W. Dijkstra, Crystal structure of Agaricus bisporus mushroom tyrosinase: identity of the tetramer subunits and interaction with tropolone, Biochemistry 50 (2011) 5477–5486.
[27] V.M. Virador, J.P. Reyes Grajeda, A. Blanco-Labra, E. Mendiola-Olaya, G.M. Smith, A. Moreno, J.R. Whitaker, Cloning, sequencing, purification, and crystal structure of Grenache (Vitis vinifera) polyphenol oxidase, J. Agric. Food Chem. 58 (2010) 1189–1201.
[28] T. Klabunde, C. Eicken, J.C. Sacchettini, B. Krebs, Crystal structure of a plant catechol oxidase containing a dicopper center, Nat. Struct. Biol. 5 (1998) 1084–1090.
[29] A. Bijelic, M. Pretzler, C. Molitor, F. Zekiri, A. Rompel, The structure of a plant tyrosinase from walnut leaves reveals the importance of "Substrate-Guiding residues" for enzymatic specificity, Angew Chem. Int. Ed. Engl. 54 (2015) 14677–14680.
[30] I. Kampatsikas, A. Bijelic, M. Pretzler, A. Rompel, A peptide-induced self-cleavage reaction initiates the activation of tyrosinase, Angew Chem. Int. Ed. Engl. 58 (2019) 7475–7479.
[31] I. Kampatsikas, A. Bijelic, A. Rompel, Biochemical and structural characterization of tomato polyphenol oxidases provide novel insights into their substrate specificity, Sci. Rep. 9 (2019) 4022.
[32] Y.C. Li, Y. Wang, H.B. Jiang, J.P. Deng, Crystal structure of *Manduca sexta* prophenoloxidase provides insights into the mechanism of type 3 copper enzymes, Proc. Natl. Acad. Sci. U. S. A. 106 (2009) 17002–17006.
[33] T. Masuda, K. Momoji, T. Hirata, B. Mikami, The crystal structure of a crustacean prophenoloxidase provides a clue to understanding the functionality of the type 3 copper proteins, FEBS J. 281 (2014) 2659–2673.
[34] Y. Hu, Y. Wang, J. Deng, H. Jiang, The structure of a prophenoloxidase (PPO) from Anopheles gambiae provides new insights into the mechanism of PPO activation, BMC Biol. 14 (2016) 2.
[35] N. Hakulinen, C. Gasparetti, H. Kaljunen, K. Kruus, J. Rouvinen, The crystal structure of an extracellular catechol oxidase from the ascomycete fungus Aspergillus oryzae, J. Biol. Inorg. Chem. 18 (2013) 917–929.
[36] M. Goldfeder, M. Kanteev, S. Isaschar-Ovdat, N. Adir, A. Fishman, Determination of tyrosinase substrate-binding modes reveals mechanistic differences between type-3 copper proteins, Nat. Commun. 5 (2014) 4505.
[37] E. Solem, F. Tuczek, H. Decker, Tyrosinase versus catechol oxidase: one asparagine makes the difference, Angew Chem. Int. Ed. Engl. 55 (2016) 2884–2888.
[38] I. Kampatsikas, A. Bijelic, M. Pretzler, A. Rompel, Three recombinantly expressed apple tyrosinases suggest the amino acids responsible for mono- versus diphenolase activity in plant polyphenol oxidases, Sci. Rep. 7 (2017) 8860.
[39] I. Kampatsikas, A. Bijelic, A. Rompel, Biochemical and structural characterization of tomato polyphenol oxidases provide novel insights into their substrate specificity, Sci. Rep. 9 (2019).
[40] T. Masuda, T. Kawauchi, Y. Yata, Y. Matoba, H. Toyohara, Two types of phenoloxidases contribute to hemolymph PO activity in spiny Lobster, Food Chem. 260 (2018) 166–173.
[41] S. Baba, T. Hoshino, L. Ito, T. Kumasaka, Humidity control and hydrophilic glue coating applied to mounted protein crystals improves X-ray diffraction experiments, Acta Crystallogr D Biol Crystallogr 69 (2013) 1839–1849.
[42] W. Kabsch, Xds, Acta Crystallogr D Biol Crystallogr 66 (2010) 125–132.
[43] A. Vagin, A. Teplyakov, MOLREP: an automated program for molecular replacement, J. Appl. Crystallogr. 30 (1997) 1022–1025.
[44] G.N. Murshudov, A.A. Vagin, E.J. Dodson, Refinement of macromolecular structures by the maximum-likelihood method, Acta Crystallogr D Biol Crystallogr 53 (1997) 240–255.
[45] P.D. Adams, R.W. Grosse-Kunstleve, L.W. Hung, T.R. Ioerger, A.J. McCoy, N.W. Moriarty, R.J. Read, J.C. Sacchettini, N.K. Sauter, T.C. Terwilliger, PHENIX: building new software for automated crystallographic structure determination, Acta Crystallogr D Biol Crystallogr 58 (2002) 1948–1954.
[46] W. Kabsch, C. Sander, Dictionary of protein secondary structure: pattern recognition of hydrogen-bonded and geometrical features, Biopolymers 22 (1983) 2577–2637.
[47] N. Ojima, K. Sakai, K. Matsuo, T. Matsui, T. Fukazawa, H. Namatame, M. Taniguchi, K. Gekko, Vacuum-ultraviolet circular dichroism spectrophotometer using synchrotron radiation: optical system and on-line performance, Chem. Lett. (2001) 522–523.
[48] K. Matsuo, K. Sakai, Y. Matsushima, T. Fukuyama, K. Gekko, Optical cell with a temperature-control unit for a vacuum-ultraviolet circular dichroism spectrophotometer, Anal. Sci. 19 (2003) 129–132.
[49] T. Masuda, R. Otomo, H. Kuyama, K. Momoji, M. Tonomoto, S. Sakai, O. Nishimura, T. Sugawara, T. Hirata, A novel type of prophenoloxidase from the kuruma prawn Marsupenaeus japonicus contributes to the melanization of plasma in crustaceans, Fish Shellfish Immunol. 32 (2012) 61–68.
[50] K. Matsuo, R. Yonehara, K. Gekko, Secondary-structure analysis of proteins by vacuum-ultraviolet circular dichroism spectroscopy, J. Biochem. 135 (2004) 405–411.
[51] K. Matsuo, R. Yonehara, K. Gekko, Improved estimation of the secondary structures of proteins by vacuum-ultraviolet circular dichroism spectroscopy, J. Biochem. 138 (2005) 79–88.
[52] N. Fujieda, A. Yakiyama, S. Itoh, Five monomeric hemocyanin subunits from Portunus trituberculatus: purification, spectroscopic characterization, and quantitative evaluation of phenol monooxygenase activity, Biochim. Biophys. Acta 1804 (2010) 2128–2135.
[53] D. Satoh, A. Horii, M. Ochiai, M. Ashida, Prophenoloxidase-activating enzyme of the silkworm, Bombyx mori. Purification, characterization, and cDNA cloning, J. Biol. Chem. 274 (1999) 7441–7453.
[54] H. Tang, Z. Kambris, B. Lemaitre, C. Hashimoto, Two proteases defining a melanization cascade in the immune system of Drosophila, J. Biol. Chem. 281 (2006) 28097–28104.
[55] H. Jiang, Y. Wang, M.R. Kanost, Pro-phenol oxidase activating proteinase from an insect, Manduca sexta: a bacteria-inducible protein similar to Drosophila easter, Proc. Natl. Acad. Sci. U. S. A. 95 (1998) 12220–12225.
[56] S. Piao, Y.L. Song, J.H. Kim, S.Y. Park, J.W. Park, B.L. Lee, B.H. Oh, N.C. Ha, Crystal structure of a clip-domain serine protease and functional roles of the clip domains, EMBO J. 24 (2005) 4404–4414.
[57] I. Kampatsikas, A. Bijelic, M. Pretzler, A. Rompel, A peptide-induced self-cleavage reaction initiates the activation of tyrosinase, Angew Chem. Int. Ed. Engl. 58 (2019) 7475–7479.
[58] K. Nellaiappan, M. Sugumaran, On the presence of prophenoloxidase in the hemolymph of the horseshoe crab, *Limulus*, Comp. Biochem. Physiol. B Biochem. Mol. Biol. 113 (1996) 163–168.
[59] T. Nagai, S. Kawabata, A link between blood coagulation and prophenol oxidase activation in arthropod host defense, J. Biol. Chem. 275 (2000) 29264–29267.
[60] E. Jaenicke, H. Decker, Conversion of crustacean hemocyanin to catecholoxidase, Micron 35 (2004) 89–90.
[61] C. Morioka, Y. Tachi, S. Suzuki, S. Itoh, Significant enhancement of monooxygenase activity of oxygen carrier protein hemocyanin by urea, J. Am. Chem. Soc. 128 (2006) 6788–6789.
[62] K. Suzuki, C. Shimokawa, C. Morioka, S. Itoh, Monooxygenase activity of *Octopus vulgaris* hemocyanin, Biochemistry 47 (2008) 7108–7115.